
Article:
A Rashid, A.S., Black, J.A., Kueh, A.B.H. et al. (2017) Bearing capacity charts of soft soil reinforced by deep mixing. Proceedings of the Institution of Civil Engineers - Ground Improvement, 170 (1). pp. 12-25. ISSN: 1755-0750

https://doi.org/10.1680/jgrim.15.00008

Ground Improvement
Volume 170 Issue GI1

Bearing capacity charts of soft soil reinforced by deep mixing
A Rashid, Black, Kueh *et al.*

ice | proceedings

Proceedings of the Institution of Civil Engineers
Ground Improvement 170 February 2017 Issue GI1
Pages 12–25 http://dx.doi.org/10.1680/jgrim.15.00008
Paper 1500008
Received 23/01/2015 Accepted 07/09/2016
Published online 12/10/2016
Keywords: composite structures/foundations/geotechnical engineering

ice Institution of Civil Engineers
publishing

Bearing capacity charts of soft soil reinforced by deep mixing

1 Ahmad Safuan A Rashid PhD
Senior Lecturer, Department of Geotechnics and Transportation, Faculty of Civil Engineering, Universiti Teknologi Malaysia, Johor, Malaysia; Fellow, Centre of Tropical Geoengineering (GEOTROPIK), Faculty of Civil Engineering, Universiti Teknologi Malaysia, Johor, Malaysia (corresponding author: ahmadsafuan@utm.my)

2 Jonathan A. Black PhD
Lecturer, Department of Civil and Structural Engineering, The University of Sheffield, Sheffield, UK

3 Ahmad Beng Hong Kueh PhD
Senior Lecturer, Construction Research Centre, Universiti Teknologi Malaysia, Johor, Malaysia

4 Hisham Mohamad PhD
Associate Professor, Civil and Environmental Engineering Department, Universiti Teknologi PETRONAS, Seri Iskandar, Perak, Malaysia

5 Norhazilan Md Noor PhD
Associate Professor, Department of Structure and Materials, Faculty of Civil Engineering, Universiti Teknologi Malaysia, Johor, Malaysia





A series of preliminary design charts were developed to predict the bearing capacity of fully and partially penetrated deep mixing (DM) of soft soil. The charts were produced by a new numerical analysis tool based on discontinuity layout optimisation (DLO) in which a previously proposed homogenisation method was used to define the improvement area. To measure the applicability of implementation of the homogenisation method in the DLO, a series of validation processes was performed against several previous studies under uniform soil strength. A new empirical solution was developed from the DLO method using the homogenisation method for the bearing capacity of soft ground under uniform soil strength, improved by the fully penetrated DM method. Results produced by the DLO approach were compared with existing analytical solutions and better agreement was found from the present model. The charts consider variation in improvement area ratio, column length and strength, and foundation width for the fully and partially penetrated DM cases. The simulations were related to real field cases in which the strength characteristics of soft soil increase with depth. An example is given to demonstrate use of the charts.

Notation

a_p	improvement area ratio
B	width of the footing
c_{ua}	average undrained shear strength of improved ground
c_{uao}	average undrained shear strength of improved ground at the top
c_{uc}	undrained shear strength of the soil–cement column
c_{us}	undrained shear strength of the surrounding soil
c_{usb}	undrained shear strength of the native soil at the bottom of the improvement area
c_{uso}	undrained shear strength of the native soil at the top of the improvement area
D	depth of improvement area
K_c	relative cohesion ratio of the column to the soft soil
L	length of the footing
N	number of measurements (sample)
N_c	bearing capacity factor
q	ultimate bearing capacity
z	depth below the soil surface

1. Introduction

Deep mixing (DM) has been commonly applied to improve soft soil ground since it was initiated approximately 30 years ago in Japan and Sweden (Porbaha, 1998). The DM method is a soil modification technique in which soil is mixed in situ with stabiliser agents in the form of slurry or powder. The main purposes of DM installation are to increase bearing capacity, control and reduce settlement, reduce the permeability of loose or compressible soil and increase the stability of soil underneath structures (Karastanev *et al.*, 1997; Porbaha, 1998;

Topolnicki, 2004). Thus far, several techniques of DM are available for field applications (block, wall, grid and group column types), the approaches of which depend on the purposes and the ground conditions. Among these soil improvement methods, the group column types remain extensively used to treat subsoil below a lightweight structure (Kitazume *et al*., 1996). In general, several factors influence the performance of the DM method, such as the percentage of improvement area ratio under the footing and the characteristics of the binder and native soil (Terashi, 2005), to name just a few. In the field, the use of square or triangular grids of single or combined columns is the common practice, offering an improvement area ratio, a_p, between 10 and 50% (CDIT, 2002; Karstunen, 1999). For the case of embankment construction, the diameter and spacing on the performance of improved ground should be considered separately rather than combining them into the improvement area ratio (Yapage and Liyanapathirana, 2014). Moreover, typical values of the soil–cement undrained shear strength, c_{uc}, are 10–50 times that of the undrained shear strength of the surrounding soil, c_{us} (Elias *et al*., 1998).

In the area of soil improvement, several studies have been devoted to DM to determine the ultimate bearing capacity of soft clay under vertical load using physical modelling, numerical modelling or full-scale field testing (Bouassida and Porbaha, 2004a, 2004b; Fang, 2006; Karastanev *et al*., 1997; Kitazume *et al*., 1996, 1999, 2000; Omine *et al*., 1999; Rashid *et al*., 2015a, 2015b; Terashi and Tanaka, 1981; Yapage *et al*., 2013, 2014; Yin and Fang, 2010). However, little effort has been directed to studying the performance and failure behaviour of fully and partially penetrated columns with different a_p and c_{uc} values in a real soil condition. Furthermore, there is no preliminary assessment technique for the feasibility of DM construction for a particular site.

Therefore, in order to fill the above-mentioned research gap, a useful series of design charts was produced in this study to facilitate the preliminary assessment and design of the bearing capacity of fully and partially penetrated DM by considering several practical guidelines of DM construction. To develop the design charts, a new numerical analysis tool, LimitState:Geo software, which is based on the discontinuity layout optimisation (DLO) procedure, was used. In addition, the homogenisation method proposed by Omine *et al*. (1999) was used for the definition of improvement area in the analysis. Before production of the design chart, a series of analyses was performed using previous studies as a comparison template (Bouassida and Porbaha, 2004a, 2004b; Omine *et al*., 1999) to validate the implementation of the homogenisation method in the software. As a result, a new empirical bearing capacity solution for the fully penetrated DM method was introduced from these analyses. The simulations were correlated to real field cases in which the strength of the soil increases with depth. An example is offered to demonstrate the applicability of the charts.

2. Discontinuity layout optimisation

The DLO procedure was first proposed by Smith and Gilbert (2007) as a new numerical limit analysis procedure for continuum mechanics. By finding an analogy between the layout optimisations of truss and plane strain plasticity problems, linear programming was used in the DLO procedure to determine the minimum upper-bound solution for a given set of potential discontinuities. The LimitState:Geo software was developed based on this method (Gilbert *et al*., 2010).

In the DLO procedure, the upper bound of the failure load is determined from an arrangement of lines of discontinuities present in the failure field of a plane plasticity problem. The procedure is analogous to the traditional upper-bound limit analysis, which identifies the optimal arrangement of sliding rigid blocks. The upper-bound limit analysis determines the bearing capacity (undrained failure) of the soil material based on the energy dissipation rate mechanism where the deformation (m) and the undrained shear strength of the soil (kN/m^2) and relative sliding velocity are considered (Powrie, 2002). Figure 1 shows the stages involved in the DLO analysis for the current work. First, for the problem idealised in Figure 1(a), a group of nodes was defined, as shown in Figure 1(b). Second, as shown in Figure 1(c), potential discontinuities, which were distributed across the problem area and were permitted to cross over one another to provide a large search space, were introduced and connected to each node. The procedure is able to model rotational as well as translational mechanisms.

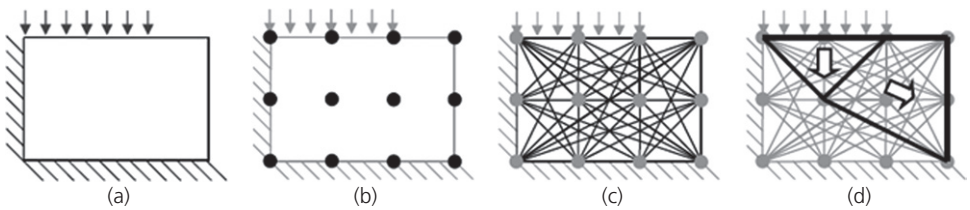

Figure 1. Stages of DLO procedure: (a) application of surcharge; (b) definition of node distribution; (c) interconnection of nodes with potential discontinuities; (d) determination of failure mechanism using optimisation (Gilbert *et al*., 2010)

Lastly, the failure mechanism was produced using a linear optimiser, as shown in Figure 1(d). The accuracy of this method depends on the node density distributed across the problem area that links the potential active discontinuities with each node. In this study, translational and rotational mechanisms were allowed along the boundaries during the analysis due to the slightly different stiffnesses of the improvement area and the surrounding soil.

3. Homogenisation method

To analyse DM using the LimitState:Geo software, a homogenisation method was used for the reinforced region (improvement area). This method was used to transform the three-dimensional problem to a two-dimensional plane strain idealisation. A structure having the same geometry as the initial unreinforced soil and subjected to the same loading conditions was defined whereby the composite reinforced material was replaced by an equivalent homogeneous material (Jellali *et al.*, 2005). An example of bearing capacity solution using different homogenisation methods is given in Figure 2. Figure 2(a) shows a block of improvement area by DM homogenised with the surrounding soil under the footing while Figure 2(b) shows three DM columns homogenised individually with the surrounding soil. They are, respectively, defined as the block and single homogenisation methods. Note that the shaded area indicates a homogenised region. Examination was carried out to determine the applicability of the two homogenisation methods in terms of determination of the bearing capacity factor, N_c (ultimate load, q_{ult}/undrained shear strength of surrounding soil, c_{us}). In the homogenisation procedure, the strength of the shaded region was determined based on the average strength of the improved ground, c_{ua}, in the out-of-plane dimension to determine the bearing capacity for the fully penetrated and floating DM method for uniform soil strength. The c_{ua} equation was derived based on the ratio of the undrained shear strength of the soil–cement column, c_{uc}, and the undrained shear strength of the unimproved ground, c_{us}, as given by

$$1. \quad c_{ua} = \left[(c_{uc} \times a_p) + \left(c_{us} \times (1 - a_p)\right)\right]$$

The white lines in Figure 2 show the failure slip mechanism generated by the LimitState:Geo software.

Using different soil–cement strengths (10–100 kPa) and improvement area ratios (10–30%), the results generated from both approaches shown in Figure 2 were compared, as shown in Figure 3. It is obvious that a very strong relationship is exhibited, with a coefficient of correlation, R^2, equal to 1. It can be concluded that the average stiffness/strength calculated from the homogenised method could provide the same result of bearing capacity although the geometry is different in the plane strain analyses. For simplicity, the block homogenisation method was chosen and used in the software in this study. The bearing capacity computed using this method will be next compared with several previous laboratory results to examine the applicability of homogenisation coupled with the DLO method.

4. Analytical description of the bearing capacity

The aim was to get a relationship between the bearing capacity factor, N_c, of the DM method with different improvement area ratios, a_p, undrained shear strengths of the soil, c_{us}, and undrained shear strengths of the soil–cement columns, c_{uc}. A strip footing of width B was considered using a fully penetrated DM method. In addition, a geometry similar to the testing chamber of Bouassida and Porbaha (2004a, 2004b), which was prescribed with a fine density of 1000 nodes, was generated. For various column strengths and improvement area ratios, the average shear strength of the improved ground underneath the footing, c_{ua}, was normalised with the undrained shear strength of the surrounding soil, c_{us}. In this study, the interface between DM columns and surrounding soils can be assumed to form a perfect bond; the validity of such behaviour has been investigated extensively through numerical methods (Yapage and Liyanapathirana, 2014).

Figure 4 shows a plot of bearing capacity factor, N_c, against the ratio c_{ua}/c_{us}, from which a linear relationship can be

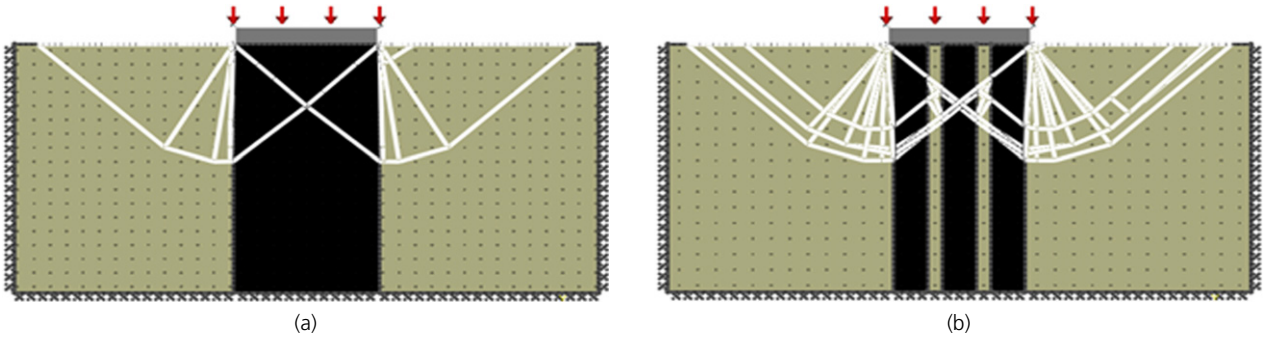

(a) (b)

Figure 2. Bearing capacity solution based on different homogenisation methods: (a) block homogenisation method; (b) single homogenisation method

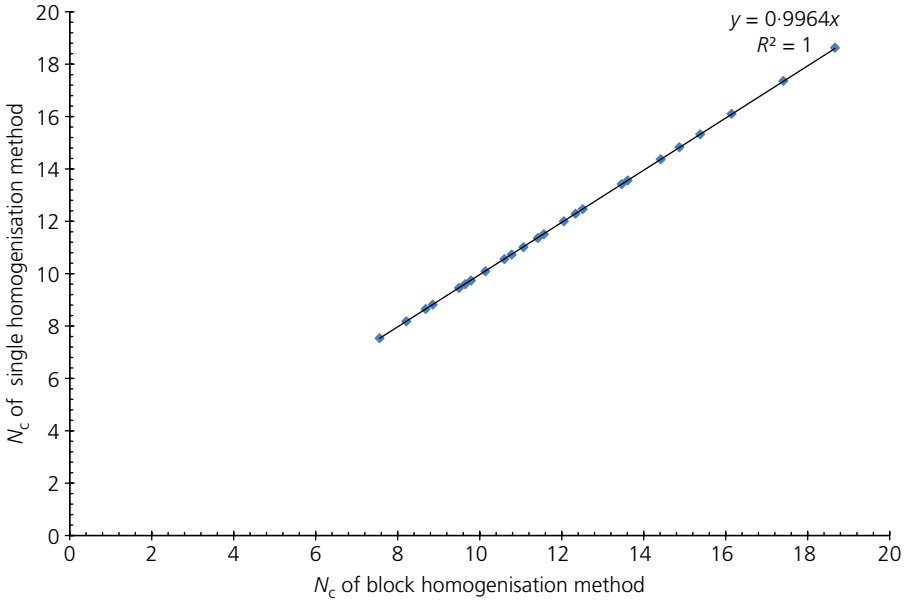

Figure 3. Correlation between block and single homogenisation methods

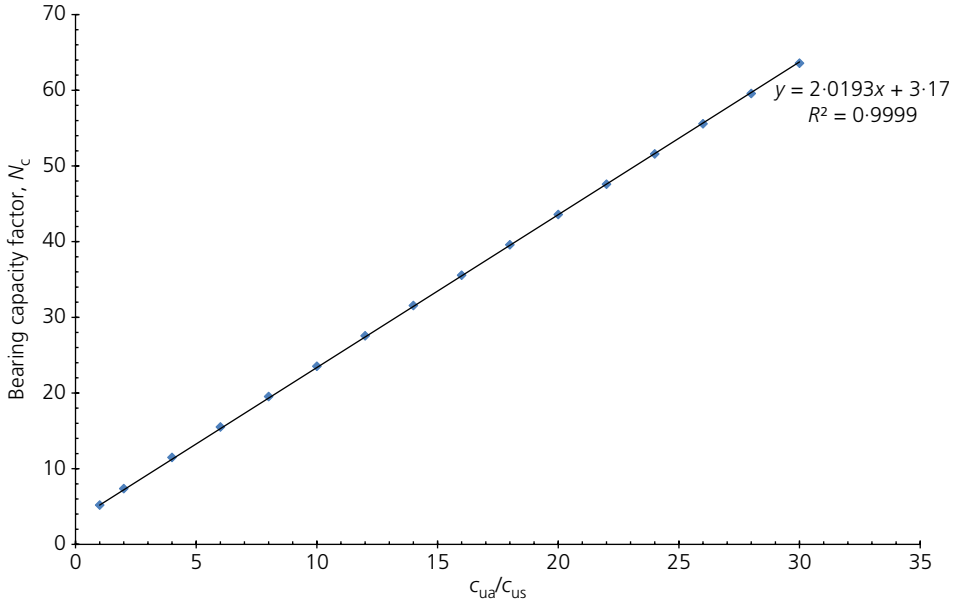

Figure 4. Relationship between N_c and c_{ua}/c_{us} obtained from LimitState:Geo

obtained as

2. $$N_{c,Eq} = 5{\cdot}19 + 2\left(\frac{c_{ua}}{c_{us}} - 1\right)$$

In comparison with the tests conducted by Bouassida and Porbaha (2004a, 2004b), a small difference of 0·9% was observed in the case of a long rectangular foundation in clay, with a bearing capacity factor of 5·14. Moreover, the sensitivity of the solution to nodal density was checked by making an increment in node number to 5000 nodes, from which only a small difference (amounting to 0·4%) was found. Following such a refinement of nodal density, the time of analysis increased. As a result, the node distribution with a coarser density was considered in all subsequent analyses since such density was evidently sufficient.

For verification, the obtained equation, Equation 2, was compared with previous laboratory results conducted by Bouassida and Porbaha (2004a, 2004b) and Omine *et al*. (1999). Tables 1 and 2 present the mechanical characteristics and the resulting N_c gained from previous laboratory studies and the present model. The cohesion of the soil–cement column, c_{uc}, was determined from the peak (yield) of the stress–strain curve obtained from the unconfined compressive strength test (Bouassida and Porbaha, 2004a; Omine *et al*., 1999). In addition, the experimental bearing capacity factor, $N_{c,Exp}$, and the calculated $N_{c,Eq}$, are listed separately in Table 3. To verify the effectiveness of Equation 2, a comparison was also made with the static (lower bound) and kinematic (upper bound) approaches of Bouassida and Porbaha (2004a, 2004b) and the method proposed by Broms (2000) using the sum of creep resistance of columns and bearing capacity of soft soil, for fully penetrated soil–cement columns. For convenience, their proposed equations are presented, respectively, below

3. $$N_{c,Static} \geq \left[4 + 2a_p(K_c - 1)\right]$$

Model	a_p: %	c_{us}: kPa	c_{uc}: kPa	K_c	q: kPa	$N_{c,Exp}$	$N_{c,Eq}$
Case 1	22·0	2·66	29·96	11·3	25·0	9·4	9·71
Case 2	42·0	2·66	29·96	11·3	39·2	14·7	14·81
Case 3	22·0	2·66	113·29	42·6	57·9	21·8	23·49

$N_{c,Exp}$, bearing capacity factor obtained from the experiments by Omine *et al*. (1999); $N_{c,Eq}$, bearing capacity factor obtained from Equation 2

Table 1. Mechanical characteristics of the scaled models of improved ground

Model	a_p: %	c_{us}: kPa	c_{uc}: kPa	K_c	q: kPa	$N_{c,Exp}$	$N_{c,Eq}$
Case A	18·8	14·1	322·0	22·8	182·0	12·9	13·05
Case B	18·8	15·7	292·0	18·6	186·7	11·9	11·53
Case C	18·8	9·4	259·0	27·2	132·7	13·8	13·55
Case D	18·8	11·0	266·5	25·4	152·0	14·1	14·75
Case E	18·8	12·6	357·0	26·1	181·3	14·4	15·03
Case F	18·8	9·5	347·5	36·6	162·7	17·1	18·00

$N_{c,Exp}$, bearing capacity factor obtained from the experiments by Bouassida and Porbaha (2004a, 2004b); $N_{c,Eq}$, bearing capacity factor obtained from Equation 2

Table 2. Mechanical characteristics of the scaled models of improved ground

4. $$N_{c,Kin} = 2\sqrt{2} + 2\sqrt{\left[1 + a_p(K_c - 1)\right]\left[2 + a_p(K_c - 1)\right]}$$

5. $$N_{c,Brm} = 1{\cdot}4a_pK_c + \lambda\left(1 + 0{\cdot}2\frac{B}{L}\right)$$

where λ is proposed as 5·5 by Bergado *et al*. (1994), B and L are, respectively, the width and length of the footing and K_c is the cohesion ratio. Overall, Equation 2 produces the smallest differences, which could be related to the variation in homogeneity (strength) of the clay bed. The root mean square error was calculated as 0·79 from Equation 2, 1·14 from Bouassida and Porbaha's static method, 1·17 from Bouassida and Porbaha's kinematic method and 1·54 from Broms' method. This means that Equation 2 is in better agreement with the laboratory results compared with other approaches.

Although both Equation 2 and Bouassida and Porbaha's kinematic approach are based on the upper-bound solution, a better result is given by Equation 2 because the DLO method considers more than five blocks of mechanism, as shown in Figure 2. Besides that, the currently proposed equation is more simplified. On the other hand, larger differences are observed in the results produced by Bouassida and Porbaha's static and Broms' methods, which are based on the lower-bound and superposition solutions. Generally, the experimental results lie between the upper-bound and lower-bound boundaries. The upper-bound solution is more realistic compared with that of Broms' (2000) because it is based on a similar failure mechanism (shallow failure), and could be used for any column reinforcement method (Bouassida and Porbaha, 2004a, 2004b).

Figure 5 shows a comparison of the predicted N_c using Equation 2, Bouassida and Porbaha's static and kinematic methods and Broms' method with previous laboratory results. Note that Equation 2 gives values almost exact to previous laboratory results for the range of $N_c = 10$–17, but shows little overprediction thereafter. For Bouassida and Porbaha's static equation, on the other hand, underprediction is demonstrated compared with previous laboratory results when $N_c = 10$–17, with good agreement thereafter. Bouassida and Porbaha's kinematic equation produces a 2·15% overprediction for the whole range of N_c, whereas Broms' equation underpredicts 2·64% of that measured.

5. Preliminary design chart

In previous sections it was shown that LimitState:Geo simulated the bearing capacity reasonably well. However, it was realised that in single gravity (1g) modelling, the strength with depth profiles did not represent typical field conditions. Therefore, further numerical analysis was carried out in which typical ground conditions were modelled. As a result, preliminary dimensionless

	Model	$N_{c,Exp}$ (a)	$N_{c,Eq}$ (b)	Difference: % (b) to (a)	$N_{c,Stat}$ (c)	Difference: % (c) to (a)	$N_{c,Kin}$ (d)	Difference: % (d) to (a)	$N_{c,Brm}$ (e)	Difference: % (e) to (a)
Omine *et al.* (1999)	Case 1	9·40	9·71	3·2	8·52	−10·4	10·28	8·5	9·94	5·4
	Case 2	14·7	13·81	−6·4	12·62	−16·5	14·41	−2·0	13·09	−12·3
	Case 3	21·8	23·49	7·2	22·30	2·2	24·10	9·6	19·59	−11·3
Bouassida and Porbaha (2004a, 2004b)	Case A	12·9	13·05	1·2	11·86	−8·8	13·64	5·4	11·67	−10·6
	Case B	11·9	11·53	−3·2	10·34	−15·1	12·11	1·7	10·60	−12·3
	Case C	14·1	13·55	−1·8	12·36	−11·6	14·15	2·4	12·02	−14·8
	Case D	13·8	14·75	4·4	13·56	−4·0	15·35	8·1	12·86	−9·7
	Case E	14·4	15·03	4·2	13·84	−4·0	15·63	7·9	13·05	−10·3
	Case F	17·1	18·00	5·0	16·81	−1·7	18·61	8·1	15·13	−13·0

$N_{c,Exp}$, bearing capacity factor obtained from experiments; $N_{c,Eq}$, bearing capacity factor obtained from Equation 2; $N_{c,Kin}$, bearing capacity factor obtained from Bouassida and Porbaha's kinematic method; $N_{c,Stat}$, bearing capacity factor obtained from Bouassida and Porbaha's static method; $N_{c,Brm}$, bearing capacity factor obtained from Broms' method

Table 3. Comparison of bearing capacity factors from Bouassida and Porbaha (2004a, 2004b) and Omine *et al.* (1999) with LimitState:Geo software and Equation 2

design charts were developed to predict the short-term behaviour, which is the bearing capacity of ground improved with DM. Further research should be carried out to validate the accuracy of these upper-bound design curves with actual field measurements and calibrate the corresponding undrained shear strengths under post-yielding effects (e.g. strain softening effect of DM columns) (Yapage *et al.*, 2013, 2014).

5.1 Soil profile

To develop the design chart, a soft clay profile, representative of typical Malaysian deposits and those found more widely in Southeast Asia, was used. Generally, a soft clay profile has an undrained shear strength that increases linearly with depth underneath a surface desiccated crust of 2–3 m thickness (Poulos, 2007). A conservative relationship (Equation 6) produced by Poulos (2007), which represents typical ground conditions of soft clay in Malaysia, was used as a guide to develop the design charts

$$6. \quad c_{us} = 10 + 1{\cdot}5z \text{ kPa}$$

where z represents the depth below the soil surface (m). In some extreme conditions, the thickness of the soft clay could reach up to 40 m. Therefore, the thickness of the soft clay layer was taken to be 40 m for the purpose of the design chart development. To cover several possible soil profiles, the multiplier of z was varied as follows

$$7. \quad c_{us} = 10 + 1{\cdot}0z \text{ kPa}$$

$$8. \quad c_{us} = 10 + 2{\cdot}0z \text{ kPa}$$

5.2 Development of design charts

To reflect typical DM construction practice, several ranges of parameters were considered in developing the design charts

- improvement area ratio, a_p: 20, 25, 30%
- cohesion ratio, $K_c = c_{uc}/c_{uso}$: 5, 10, 20, 40, 60, 80, 100
- depth of the improvement area/breadth of the foundation, D/B: 0·25, 0·50, 0·75, 1·0, 1·5, 2·0, 2·5, 3·0, 4·0, 5·0.

Dimensionless design charts were developed after introducing a dimensionless parameter, K, by dividing the undrained shear strength of the native soil at the bottom of the improvement area, c_{usb}, with the undrained shear strength of the native soil at the top, c_{uso}

$$9. \quad K = \frac{c_{usb}}{c_{uso}}$$

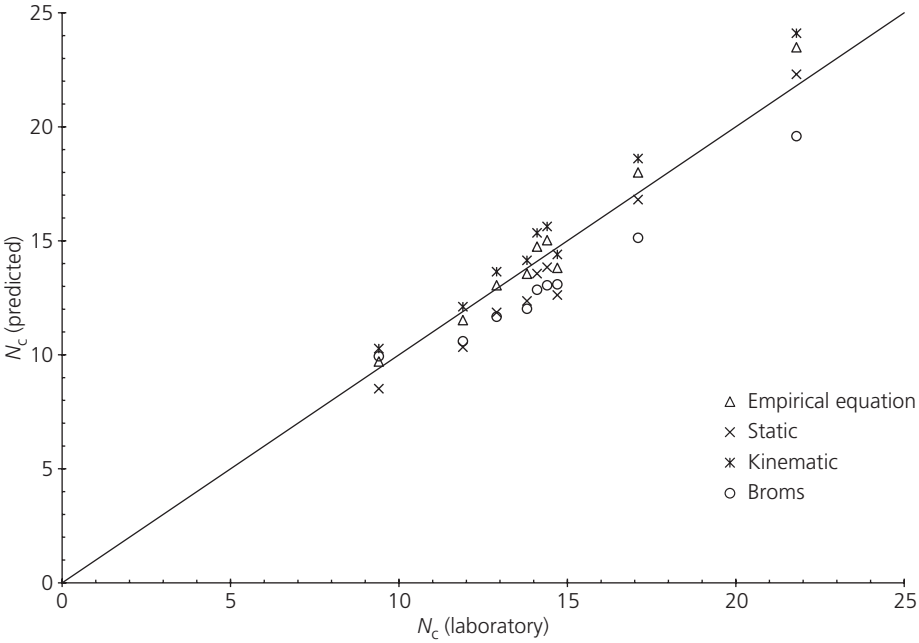

Figure 5. Comparison of N_c obtained from laboratory tests and predictions

In total, three K values ($K = 5{\cdot}0$, $7{\cdot}0$ and $9{\cdot}0$) were introduced for the fully penetrated case and seven K values ($K = 2{\cdot}0$, $2{\cdot}5$, $3{\cdot}0$, $4{\cdot}0$, $5{\cdot}0$, $5{\cdot}5$ and $7{\cdot}0$) for the partially penetrated case.

5.3 Analysis procedure

LimitState:Geo was used to perform the analysis with the baseline nodal spacing in the soil and on the boundary of 0·6 and 0·3 m, respectively. Generally, the number of nodes was around 1300 on average. The lateral boundaries of the model were extended to avoid boundary resistance to failure. In total, 2700 cases were considered to develop the design charts. The block homogenisation method (as shown in Figure 2(a)) was employed for simplicity in performing the analysis. The rigid footing width, B, was set as 10 m with a variation in D in accordance with the change in D/B ratio as mentioned in the previous section.

The charts for the fully penetrated ($K = 5$) and partially penetrated cases ($K = 5$, $D/B = 2$) were first plotted with different c_{uso}. It was found that all the results located on the same line, as shown in Figure 6(a) for the relationship between N_c and c_{uao}/c_{uso} for the fully penetrated case. Figures 6(b) and 6(c) show the comparison of the relationship between N_c and c_{uao}/c_{uso} for the partially penetrated case ($D/B = 2$, $K = 5$) for different c_{uso} and B, respectively. The above-mentioned results imply that the use of the dimensionless approach is valid for various scales and values of c_{uso}.

5.4 Design graph for fully penetrated case

Figure 7 shows the relationship between c_{uao}/c_{uso} and N_c for different K values for the fully penetrated case. It is apparent that linear relationships can be established for different K values, with a good R^2 of >0·99. The bearing capacity of the improved area relies on the stiffness of the column due to the end of the improved area meeting the hard layer (Rashid *et al.*, 2015a). These relationships are presented below for $K = 5{\cdot}0$, $7{\cdot}0$ and $9{\cdot}0$, respectively

$$N_{c,Eq} = 6{\cdot}90 + 2{\cdot}06\left(\frac{c_{uao}}{c_{uso}} - 1\right) \quad (10)$$

$$N_{c,Eq} = 7{\cdot}52 + 2{\cdot}10\left(\frac{c_{uao}}{c_{uso}} - 1\right) \quad (11)$$

$$N_{c,Eq} = 8{\cdot}08 + 2{\cdot}13\left(\frac{c_{uao}}{c_{uso}} - 1\right) \quad (12)$$

5.5 Design graph for partially penetrated case

Non-linear relationships between c_{uao}/c_{uso} and N_c were established for different K values, as shown in Figures 8–14, for the partially penetrated case for numerous D/B. It was found that, in general, N_c for the lowest D/B initiates at a higher value compared with the rest. It is believed that the strength of the native soil contributes to this result, because the strength at a

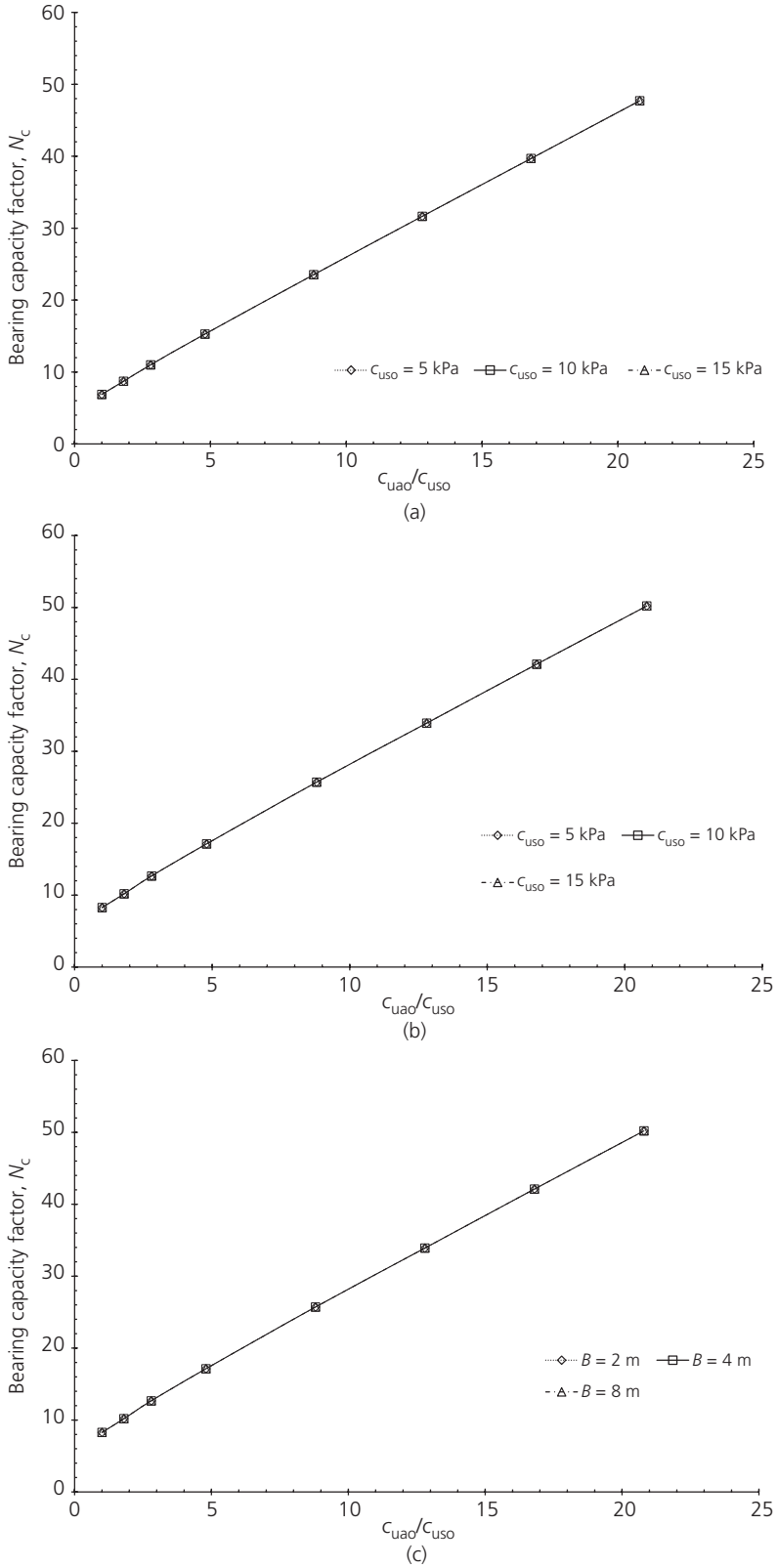

Figure 6. Comparison between N_c and c_{uao}/c_{uso} for different B (for partially penetrated, $D/B = 2$ and $K = 5{\cdot}0$): (a) fully penetrated; (b) partially penetrated (different c_{uso}, $D/B = 2$); (c) partially penetrated (different B, $D/B = 2$)

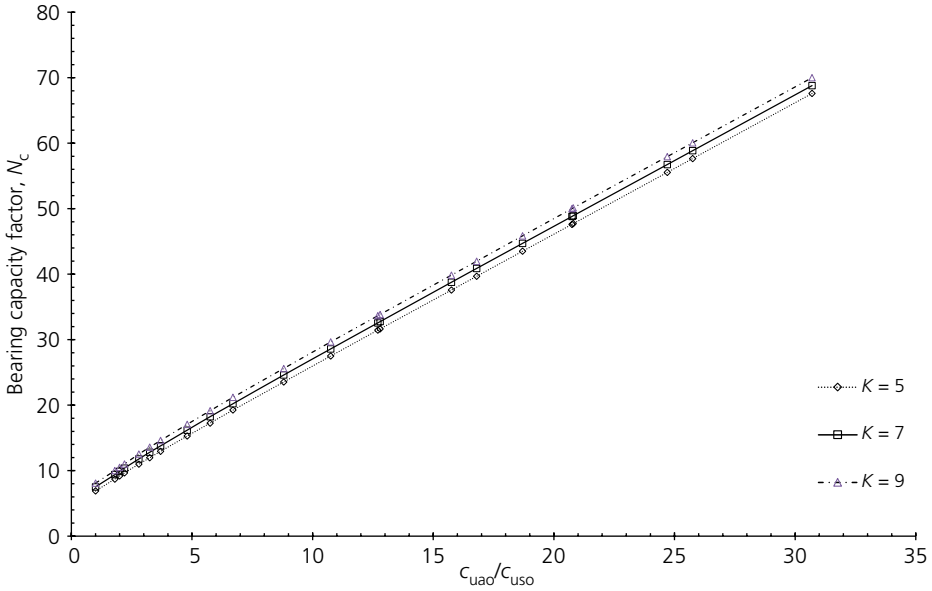

Figure 7. Relationship between N_c and c_{uao}/c_{uso} obtained from LimitState:Geo for the fully penetrated case

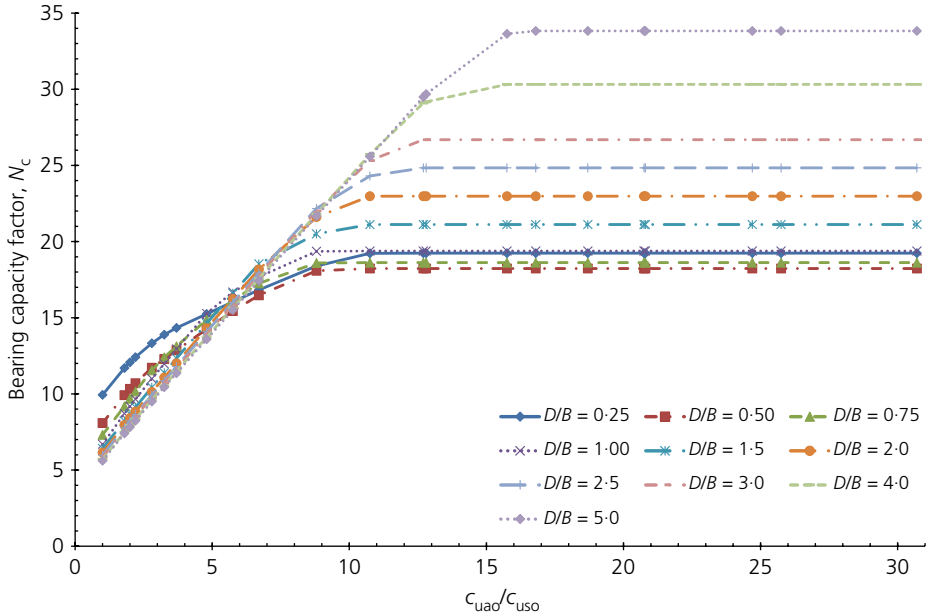

Figure 8. Relationship between N_c and c_{uao}/c_{uso} obtained from LimitState:Geo ($K = 2{\cdot}0$) for the partially penetrated case

given absolute depth (> zero) for soil with the lowest D/B is greater than the strength of those with higher D/B, according to the definition of K. Generally, the curves intersect at a certain ratio of c_{uao}/c_{uso}. Beginning from this point, the curves for soils with higher D/B display higher N_c. In some cases, the curves plateau after this intersection point. A simple design example of the application of the design charts is now presented to demonstrate its practicality.

5.6 Design example

In this example, a deep soft deposit reinforced with partially penetrated DM columns is assumed to be 12 m wide and 18 m deep. The target N_c value is 32. The improvement area ratio, a_p, is assumed to be 30% and the undrained shear strength of the columns, c_{uc}, is 700 kPa. The soft clay profile has an undrained shear strength that increases linearly with depth in accordance with $c_{us} = 10 + 1{\cdot}1z$ kPa. From this

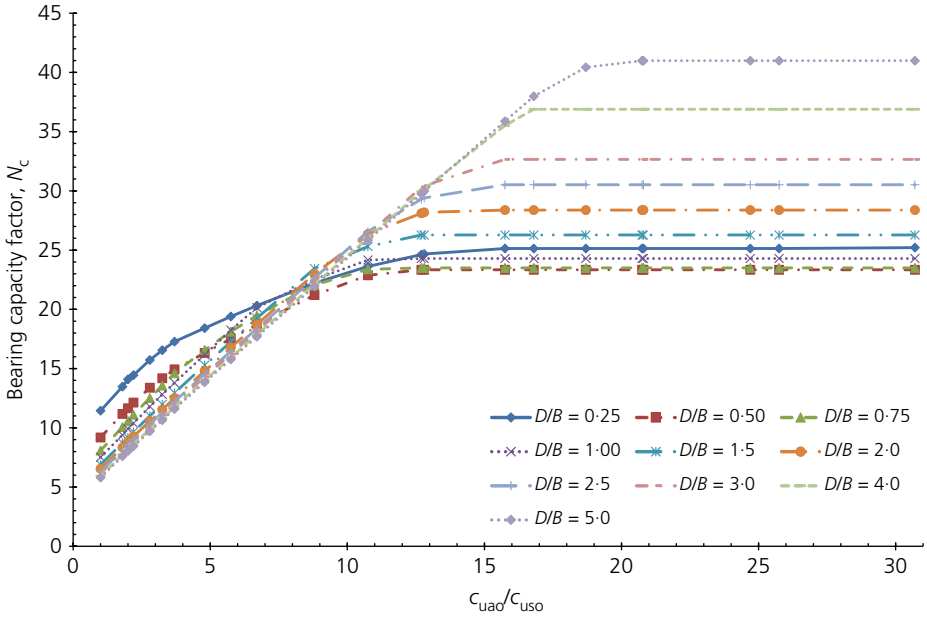

Figure 9. Relationship between N_c and c_{uao}/c_{uso} obtained from LimitState:Geo for the partially penetrated case ($K = 2{\cdot}5$)

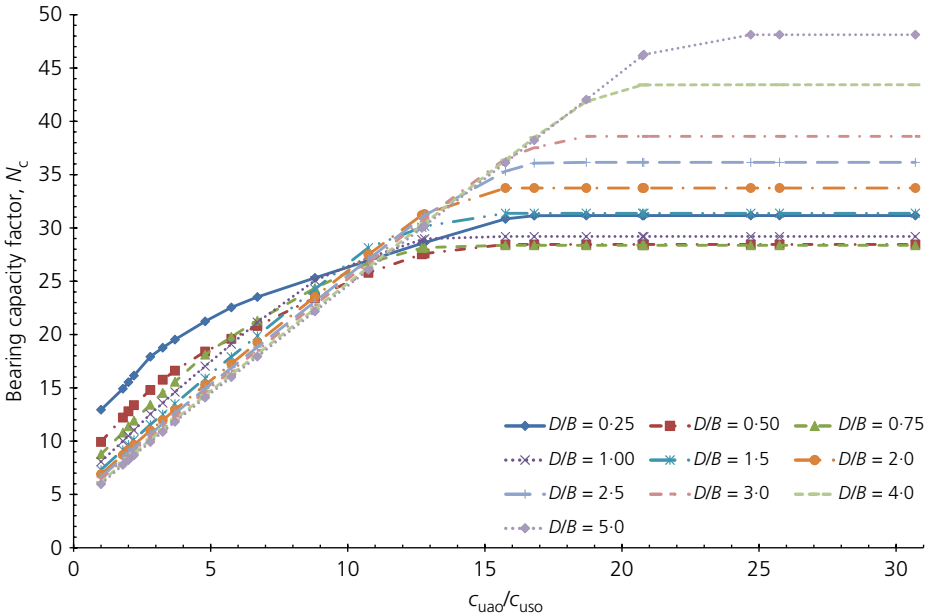

Figure 10. Relationship between N_c and c_{uao}/c_{uso} obtained from LimitState:Geo for the partially penetrated case ($K = 3{\cdot}0$)

strength relationship, the strength of the native soil at the base of the improvement ground is 30 kPa and, by using Equation 9, $K = 3$. As a result, Figure 10 will be used to predict the N_c value for the improved ground. With a D/B value of 1·5 and $c_{uao}/c_{uso} = [(0{\cdot}3 \times 700) + (0{\cdot}7 \times 10)]/10) = 21{\cdot}7$, N_c of the improved ground is 31·4. From an economics point of view, contractors could reduce the cost during construction by reducing c_{uao}/c_{uso} to 16, giving the same N_c value. They could choose to either decrease the column strength from 700 kPa to 300 kPa by decreasing the cement content or decrease the improvement area ratio from 30 to 12·9%.

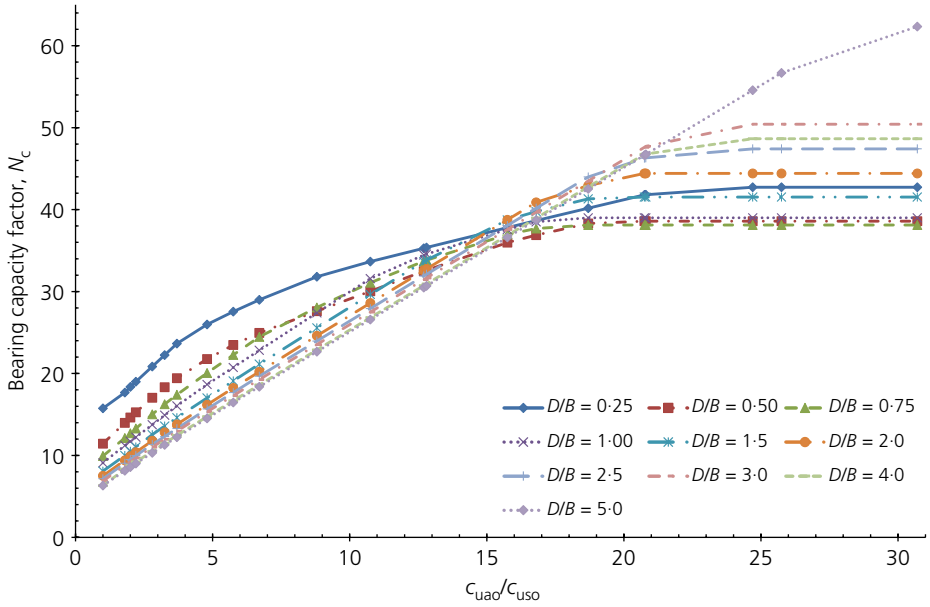

Figure 11. Relationship between N_c and c_{uao}/c_{uso} obtained from LimitState:Geo for the partially penetrated case ($K = 4{\cdot}0$)

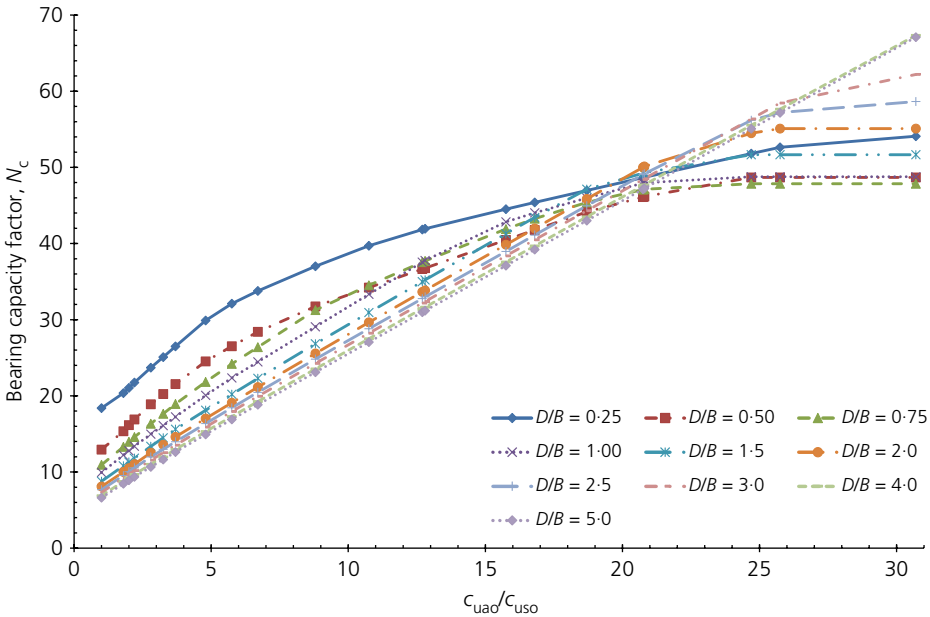

Figure 12. Relationship between N_c and c_{uao}/c_{uso} obtained from LimitState:Geo for the partially penetrated case ($K = 5{\cdot}0$)

6. Conclusions

A numerical model based on the discontinuity layout optimisation (DLO) approach coupled with a homogenisation method, which was verified with existing laboratory results, was used to produce a series of preliminary design charts for soils reinforced by the deep mixing (DM) method using fully and partially penetrated soil–cement columns. The conclusions drawn from the current study are as follows.

- A strong correlation was established between the block and individually homogenised methods using the LimitState: Geo software.

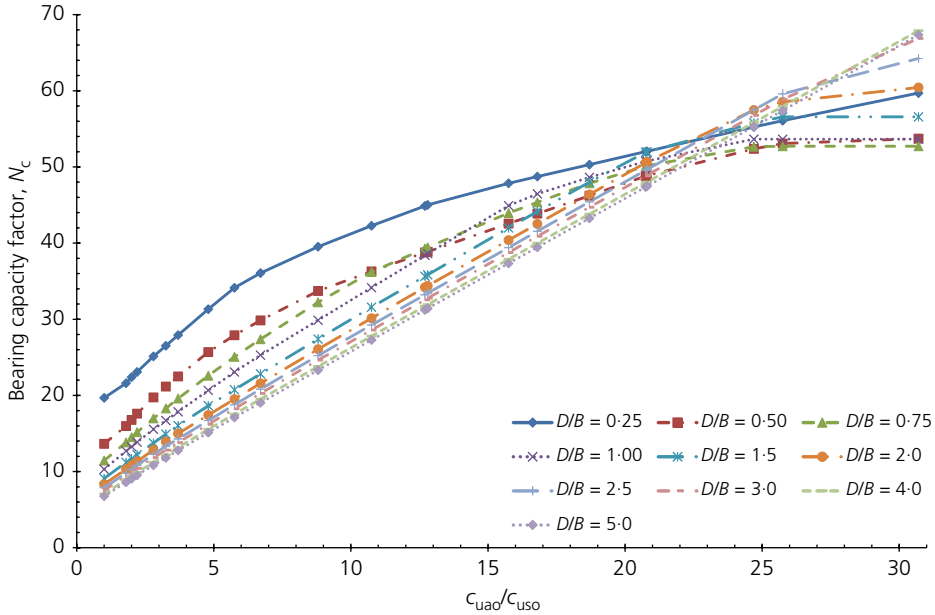

Figure 13. Relationship between N_c and c_{uao}/c_{uso} obtained from LimitState:Geo for the partially penetrated case ($K = 5{\cdot}5$)

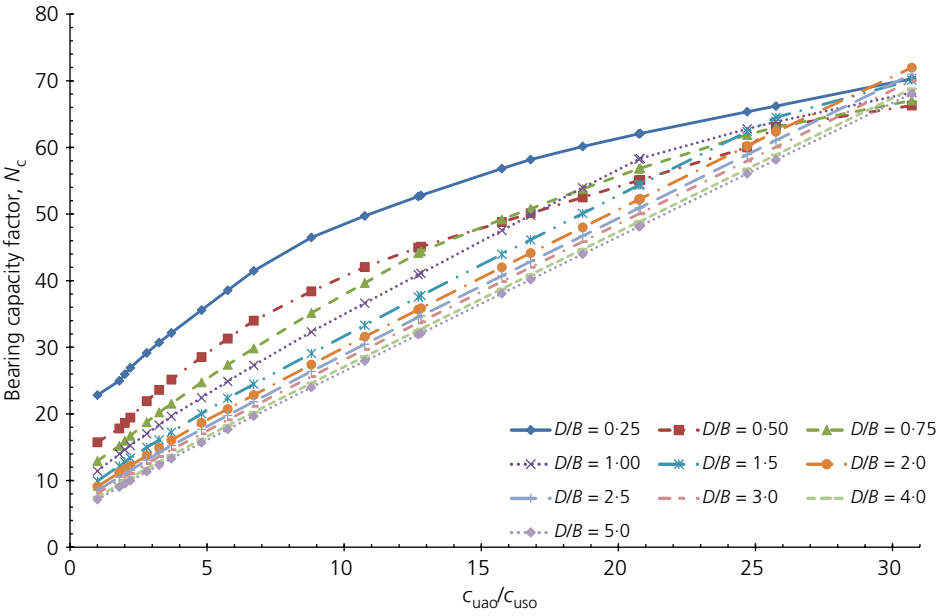

Figure 14. Relationship between N_c and c_{uao}/c_{uso} obtained from LimitState:Geo for the partially penetrated case ($K = 7{\cdot}0$)

- An equation was empirically determined as $N_{c,Eq} = 5{\cdot}19 + 2(c_{ua}/c_{us} - 1)$ using results computed by the LimitState:Geo software based on the average improvement soil strength for the fully penetrated DM under uniform soil strength. By comparing the results with previous laboratory works conducted by Bouassida and Porbaha (2004a, 2004b) and Omine *et al.* (1999), the capability of the proposed equation in determining the bearing capacity of fully penetrated soil was evident. Furthermore, the equation provides better agreement with experimental results compared with the existing equations proposed by Bouassida and Porbaha (2004a, 2004b) and Broms (2000).
- A set of preliminary design charts for practical use was developed using the results computed by the

LimitState:Geo software. These charts, which are dimensionless, reflect typical DM construction in practice, with the inclusion of parameters such as the improvement area ratio, cohesion ratio and depth of the improvement area/breadth of the foundation. In total, three K values ($K = 5{\cdot}0$, $7{\cdot}0$ and $9{\cdot}0$) were used for the fully penetrated case and seven K values ($K = 2{\cdot}0$, $2{\cdot}5$, $3{\cdot}0$, $4{\cdot}0$, $5{\cdot}0$, $5{\cdot}5$ and $7{\cdot}0$) for the partially penetrated case.

- Linear and non-linear relationships of N_c versus c_{uao}/c_{uso} were found for soils reinforced with fully and partially penetrated methods, respectively.
- For the partially penetrated case, soils with lower D/B gave higher N_c values before the intersection of design curves and vice versa.
- The preliminary design charts could provide an early prediction of the bearing capacity of soils reinforced by the DM method and could help contractors to reduce the cost of construction, as discussed in the given example.

In the future, in order to produce a more comprehensive design chart for the DM method, further work may include calibration and improvements of the upper-bound curves by considering both peak and residual undrained shear strengths of DM columns that can match field measurements with observed soil settlements.

Acknowledgements

The authors acknowledge the financial support for this research provided by the Ministry of Science and Technology of Malaysia, MOSTI, under Science Fund grant (R.J130000.7922.4S051). The authors also acknowledge the Taylor & Francis Group for providing permission to reproduce a figure from Gilbert *et al*. (2010) as Figure 1 in this paper.

REFERENCES

Bergado DT, Anderson LR, Miura N and Balasubramaniam AS (1994) Lime/cement deep mixing method. *Improvement Techniques of Soft Ground in Subsiding and Lowland Environments* (Bergado DT, Chai JC, Alfaro MC and Balasubramaniam AS (eds)). Balkelma, Rotterdam, the Netherlands, pp. 99–130.

Bouassida M and Porbaha A (2004a) Ultimate bearing capacity of soft clays reinforced by a group of columns-application to a deep mixing technique. *Soils and Foundations* **44(3)**: 91–101.

Bouassida M and Porbaha A (2004b) Bearing capacity of foundations resting on soft ground improved by soil cement columns. *Proceedings of International Conference on Geotechnical Engineering (ICGE 2004)*. Sharjah, United Arab Emirates, pp. 173–180.

Broms BB (2000) Lime and lime/columns. Summary and visions. *Proceedings of the 4th International Conference on Ground Improvement Geosystems*. Finnish Geotechnical Society, Helsinki, Finland, vol. 1, pp. 43–93.

CDIT (Coastal Development Institute of Technology) (2002) *The Deep Mixing Method – Principle, Design and Construction*. Balkelma, Rotterdam, the Netherlands.

Elias V, Welsh J, Warren J and Lukas R (1998) *Ground Improvement Technical Summaries. Volume II, Demonstration Project 116*. U.S. Department of Transportation, Federal Highway Administration, Washington, DC, USA, Publication No. FHWA-SA-98-086.

Fang Z (2006) *Physical and Numerical Modelling of the Soft Soil Ground Improved by Deep Cement Mixing Method*. PhD thesis, The Hong Kong Polyechnic University, Hong Kong.

Gilbert M, Smith C, Haslam I and Pritchard T (2010) Application of discontinuity layout optimization to geotechnical limit. *Proceedings of the 7th European Conference on Numerical Methods in Geotechnical Engineering, Trondheim, Norway*, pp. 169–174.

Jellali B, Bouassida M and de Buhan P (2005) A homogenization method for estimating the bearing capacity of soils reinforced by columns. *International Journal for Numerical and Analytical Method in Geomechanics* **29(10)**: 989–1004.

Karastanev D, Kitazume M, Miyajima S and Ikeda T (1997) Bearing capacity of shallow foundations on column type DMM improved ground. *Proceedings of the 14th International Conference on SMFE, Hamburg, Germany*, vol. 3, pp. 721–724.

Karstunen M (1999) Alternative ways of modelling embankments on deep-stabilized soil. *Proceedings of International Conference on Dry Mix Methods for Deep Soil Stabilization, Stockholm, Sweden*, pp. 221–228.

Kitazume M, Ikeda T, Miyajima S and Karastanev D (1996) Bearing capacity of improved ground with column type DMM. *Proceedings of the 2nd International Conference on Ground Improvement Geosystems, Tokyo, Japan*, vol. 1, pp. 503–508.

Kitazume M, Yamamoto M and Udaka Y (1999) Vertical bearing capacity of column type DMM ground with low improvement ratio. *Proceedings of International Conference on Dry Mix Methods for Deep Soil Stabilization, Stockholm, Sweden*, pp. 245–250.

Kitazume M, Okano K and Miyajima S (2000) Centrifuge model tests on failure envelope of column type deep mixing method improved ground. *Soils and Foundations* **40(4)**: 43–55.

Omine K, Ochiai H and Bolton MD (1999) Homogenization method for numerical analysis of improved ground with cement-treated soil columns. *Proceedings of International Conference on Dry Mix Methods for Deep Soil Stabilization, Stockholm, Sweden*, pp. 161–168.

Porbaha A (1998) State of the art in deep mixing technology: part I. Basic concepts and overview. *Proceedings of the Institution of Civil Engineers – Ground Improvement* **2(2)**: 81–92, http://dx.doi.org/10.1680/gi.1998.020204.

Poulos HG (2007) Design charts for piles supporting embankments on soft clay. *Journal of Geotechnical and Geoenvironmental Engineering* **133(5)**: 493–501.

Powrie W (2002) *Soil Mechanics: Concepts and Applications*. Spon Press, London, UK.

Rashid AAS, Black JA, Mohamad H and Mohd Noor N (2015a) Behavior of weak soils reinforced with end-bearing soil–cement columns formed by the deep mixing method. *Marine Georesources and Geotechnology* **33(6)**: 473–486.

Rashid AAS, Black JA, Kueh ABH and Md Noor N (2015b) Behaviour of weak soils reinforced with soil cement columns formed by the deep mixing method: rigid and flexible footings. *Measurement: Journal of the International Measurement Confederation* **68**: 262–279.

Smith C and Gilbert M (2007) Application of discontinuity layout optimization to plane plasticity problems. *Proceedings of the Royal Society A* **463(2086)**: 2461–2484.

Terashi M (2005) Keynote lecture: design of deep mixing in infrastructure applications. *Proceedings of International Conference on Deep Mixing – Best Practice and Recent Advances, Stockholm, Sweden*, pp. K25–K45.

Terashi M and Tanaka H (1981) Ground improved by deep mixing method. *Proceedings of the 10th ICSMFE, Stockholm, Sweden*, vol. 3, pp. 777–780.

Topolnicki M (2004) *In Situ Soil Mixing. Ground Improvement*. Spon Press, New York, NY, USA, pp. 331–428.

Yapage NNS and Liyanapathirana DS (2014) A parametric study of geosynthetic-reinforced column-supported embankments. *Geosynthetics International* **21(3)**: 213–232, http://dx.doi.org/10.1680/gein.14.00010.

Yapage NNS, Liyanapathirana DS, Poulos HG, Kelly RB and Leo CJ (2013) Numerical modeling of geotextile-reinforced embankments over deep cement mixed columns incorporating strain-softening behavior of columns. *International Journal of Geomechanics* **15(2)**: 04014047.

Yapage NNS, Liyanapathirana DS, Kelly RB, Poulos HG and Leo CJ (2014) Numerical modeling of an embankment over soft ground improved with deep cement mixed columns: case history. *Journal of Geotechnical and Geoenvironmental Engineering* **140(11)**: 04014062.

Yin JH and Fang Z (2010) Physical modeling of a footing on soft soil ground with deep cement mixed soil columns under vertical loading. *Marine Georesources and Geotechnology* **28(2)**: 173–188.